

Coherence protection in coupled quantum systems

H. M. Cammack,¹ P. Kirton,¹ P. R. Eastham,² J. Keeling,¹ and B. W. Lovett¹

¹*SUPA, School of Physics and Astronomy, University of St. Andrews, KY16 9SS, U.K.*

²*School of Physics and CRANN, Trinity College Dublin, Dublin 2, Ireland.*

The interaction of a quantum system with its environment causes decoherence, setting a fundamental limit on the suitability of a system for quantum information processing. However, we show that if the quantum system consists of coupled parts with different internal energy scales then the interaction of one part with a thermal bath need not lead to loss of coherence from the other. Remarkably, we find that the protected part can become *more* coherent when the coupling to the bath becomes stronger or the temperature is raised. Our theory will enable the design of decoherence-resistant hybrid quantum computers.

Quantum decoherence describes the process by which a small system becomes entangled with a large environment, such that its phase can no longer be defined locally [1–3]. Indeed, a single quantum system coupled weakly to a lower energy bosonic bath must lose coherence in its energy eigenbasis [4, 5]. In some sense the bath makes a ‘measurement’ of the system, and its state becomes mixed. However, the case of hybrid quantum system — i.e. one that is composed of multiple interacting parts — is much more subtle. When the constituent parts have distinct energy scales, a bath can couple to each part with a different strength, and the decoherence of one part can influence the coherence of other parts.

In this Letter, we will explore how this interplay of intra-system and system-bath coupling can affect the coherence of one part of a coupled system. In particular, we will explore whether conditions exist under which such coherence can be protected from bath-induced noise. The system we will study consists of two qubits with energy scales differing by at least one order of magnitude (see Fig. 1). The theory we discuss is generally applicable, and could apply for example to exciton-electron spin hybrids in quantum dots [6, 7], molecular systems [8] or defects in crystals [9], or to superconducting qubits coupled to spins [10] or defect centres [11]. However, we will base our argument on the concrete example of a coupled spin-half electron and spin-half nucleus [12]. Such a system has been proposed as a hybrid quantum computing device [13] represented by donors in silicon [14, 15] that can use different degrees of freedom to perform different tasks more efficiently than if a single qubit was used. Electron spins have rapid manipulation times, and these can be coupled to optical photons or superconducting qubits for measurement or entanglement [12, 13], and coupling between electron and nuclear spins provides access to quantum memory with ultra long nuclear coherence times of up to six hours [16].

As an illustrative example, we will use a simplified description in which the electron spin decays by emitting energy into a large environment (see for example [17] for a situation in which photon emission dominates spin decay), but the nucleus only interacts with the electron.

This coupling takes a form such that the transition energy of the electron has a different value for each of the two nuclear spin states. We might then expect that the rate of electron spin decay would have a profound effect on whether or not the environment destroys coherent superpositions of nuclear states by projecting the nucleus onto one of its energy eigenstates. For a sufficiently slow decay at low temperature, the different nuclear spin states would have resolved lines in the electron spin emission spectrum, and we will argue this leads to a loss of nuclear coherence (see Fig. 1). Conversely, we will investigate whether a fast electron spin decay is able to preserve nuclear spin coherence. We will finally explore the impact of increasing temperature on these findings.

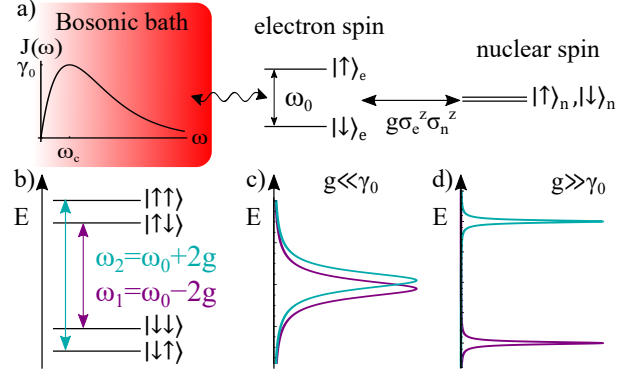


FIG. 1. a) A coupled nuclear-electron spin system with electron Zeeman splitting of ω_0 and hyperfine coupling g . We neglect the Zeeman splitting of the nuclear spin, and only the electron interacts with a thermal reservoir. b) The eigenenergies of the two-spin system and allowed transitions $\omega_{1,2}$. When the hyperfine coupling is small (c), the transitions overlap and nuclear spin coherences can survive. Increasing the hyperfine coupling (d) resolves the transition lines and coherences are lost.

We first discuss the behavior at zero temperature. In this limit, the problem can be solved exactly. To extend our discussion to finite temperatures, we must later introduce an approximate method, and we use a Markovian quantum master equation (MQME), making approxima-

tions which are valid for the parameters we consider. By comparison to the exact solution at zero temperature, we may also directly verify that the MQME accurately predicts the residual coherence, giving confidence in the extension to non-zero temperatures. Using the MQME, the dependence of the long-time nuclear coherence on the decay rate of the electron spin will be presented and discussed, and we will suggest an experimental setup that would be capable of testing our predictions.

Our model system is depicted in Fig. 1 and is described by a total Hamiltonian $H = H_S + H_{SB} + H_B$:

$$\begin{aligned} H_S &= \frac{\omega_0}{2} \hat{\sigma}_e^z + g \hat{\sigma}_e^z \hat{\sigma}_n^z, \\ H_{SB} &= \sum_k c_k (\hat{\sigma}_e^+ \hat{b}_k + \hat{\sigma}_e^- \hat{b}_k^\dagger), \\ H_B &= \sum_k \omega_k \hat{b}_k^\dagger \hat{b}_k, \end{aligned} \quad (1)$$

where ω_0 is the electron Zeeman splitting and g is the hyperfine coupling strength. We ignore the nuclear Zeeman splitting which is negligible on this scale, and including it would have no impact on our conclusions. The environment, which couples only to the electron, is modelled as a collection of quantum harmonic oscillators where a quantum in mode k is created with b_k^\dagger . The effects of the environment are characterised by the spectral density $J(\omega) = \pi \sum_k |c_k|^2 \delta(\omega - \omega_k)$. When calculating numerical results, we use a spectral density of Ohmic form, $J(\omega) = \gamma_0 (\omega/\omega_c) \exp(1 - (\omega/\omega_c))$, where ω_c is a cutoff frequency and γ_0 is the peak spectral density. We choose $\omega_c = \omega_0$ throughout as the bath is approximately flat around the peak at $\omega = \omega_c$. In the following calculations we will switch to the interaction picture with respect to $H_0 = H_S + H_B$.

We first present the exact (non-Markovian) zero-temperature solution using the Wigner-Weisskopf method [18, 19]). Since the bath is at $T = 0$ and the Hamiltonian is number conserving we may work in the subspace where there is a single excitation in either the electron spin or bath. Therefore, a general state at time t can be written:

$$\begin{aligned} |\Psi(t)\rangle &= +a_1(t) |\uparrow\downarrow\rangle \otimes |0\rangle_B + a_2(t) |\uparrow\uparrow\rangle \otimes |0\rangle_B \\ &+ \sum_k \alpha_{1,k}(t) |\downarrow\downarrow\rangle \otimes |k\rangle_B + \alpha_{2,k}(t) |\downarrow\uparrow\rangle \otimes |k\rangle_B. \end{aligned}$$

Here the system state is given in terms of the eigenstates of $\hat{\sigma}_z$ ($|\uparrow\rangle, |\downarrow\rangle$) and with the electron spin specified first and the nuclear spin second. The state $|0\rangle_B$ is the vacuum state of the bath and $|k\rangle_B$ refers to the k th bath mode containing the excitation. We then use the Schrödinger equation to obtain differential equations for state coefficients, $\alpha_{1,k}, \alpha_{2,k}, a_1$ and a_2 . After Laplace transforming we find the equation for the states with an electronic excitation,

$$\tilde{a}_m(s)(s + f(s - i\omega_m)) = a_m(0), \quad (2)$$

where we denote Laplace transformed functions with a tilde. $m \in \{1, 2\}$ and the transition frequencies are $\omega_1 = \omega_0 - 2g$, $\omega_2 = \omega_0 + 2g$ (as depicted in Fig. 1), and

$$f(s) \equiv \sum_k \frac{|c_k|^2}{s + i\omega_k} = \frac{1}{\pi} \int_0^\infty d\nu \frac{J(\nu)}{s + i\nu}. \quad (3)$$

Eq. (2) further allows us to write:

$$\tilde{a}_{m,k}(s) = -\frac{ic_k}{s} \frac{a_m(0)}{s + i(\omega_m - \omega_k) + f(s - i\omega_k)}. \quad (4)$$

We can now find the coherence between nuclear spin levels when the electron spin has decayed to its ground state $\langle \downarrow\downarrow | \rho(t) | \downarrow\uparrow \rangle = \rho_{\downarrow\downarrow, \downarrow\uparrow}(t) = \sum_k \alpha_{1,k}(t) \alpha_{2,k}^*(t)$. Using the inverse Laplace transform of Eq. (4) yields:

$$\begin{aligned} \rho_{\downarrow\downarrow, \downarrow\uparrow}(t) &= -\frac{1}{4\pi^3} \int_{\mathcal{B}} ds_1 \int_{\mathcal{B}} ds_2 e^{(s_1 + s_2)t} a_1(0) a_2^*(0) \\ &\times \int_0^\infty d\nu J(\nu) \frac{1}{s_1(s_1 + i(\omega_1 - \nu) + f(s_1 - i\nu))} \\ &\times \frac{1}{s_2(s_2 - i(\omega_2 - \nu) + f^*(s_2 - i\nu))}, \end{aligned} \quad (5)$$

where \mathcal{B} denotes the Bromwich contour. Each of the s -integrals contains a pole at zero, and other structure (poles or branch cuts) elsewhere in the complex plane. In the long time limit, the only surviving contributions are from the $s = 0$ poles. To evaluate the residue at $s = 0$, we must find $f(-i\nu + 0_+)$. Using Eq. (3):

$$f(-i\nu + 0_+) = J(\nu) - \frac{i}{\pi} \mathcal{P} \int_0^\infty dx \frac{J(x)}{x - \nu} \equiv \Gamma(\nu), \quad (6)$$

leading to:

$$\begin{aligned} \lim_{t \rightarrow \infty} \rho_{\downarrow\downarrow, \downarrow\uparrow}(t) &= a_1(0) a_2^*(0) \frac{1}{\pi} \\ &\times \int_0^\infty d\nu \frac{J(\nu)}{(\omega_1 - \nu - i\Gamma(\nu))(\omega_2 - \nu + i\Gamma^*(\nu))}. \end{aligned} \quad (7)$$

Following preparation in the initial state $|\psi(0)\rangle = |\uparrow\rangle(|\downarrow\rangle + |\uparrow\rangle)/\sqrt{2}$, we plot the exact steady-state coherence in Fig. 2 for an Ohmic spectral density with peak at the bare electron splitting ($\omega_0 = \omega_c$). When g is small compared with the typical electronic decay rate γ_0 , nuclear coherence is preserved close to its maximum value of $1/2$ throughout the electronic decay process. Increasing g causes a reduction and eventual loss of nuclear coherence, with the effect more pronounced for smaller electron-bath coupling rates. Increasing coupling to the bath broadens the range of g over which this loss of coherence occurs, so that at fixed g , increasing damping causes increased coherence.

To see why this is, consider how the initial state $|\psi(0)\rangle$ reaches equilibrium. Our theory applies to any bosonic bath but to give a concrete illustration, we imagine that

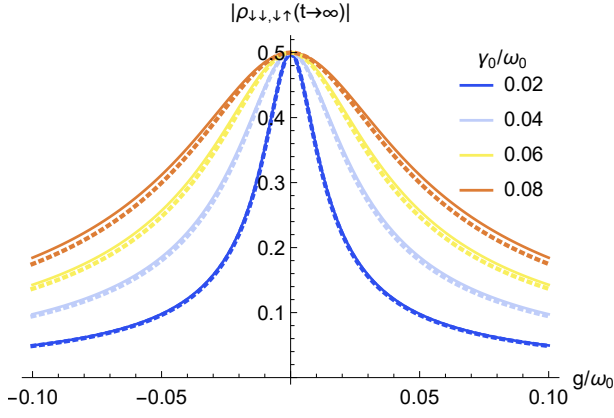


FIG. 2. The magnitude of the steady state coherence in the lower electron state, $\rho_{\downarrow,\downarrow\uparrow}$, at zero temperature as a function of the spin-spin coupling, g . The bath has an Ohmic spectral density on resonance with the bare electron splitting and peak rate γ_0 . Solid lines represent the exact solutions, whilst dashed lines show the solutions using the Born-Markov approximation.

the bath corresponds to photon modes, and so describes photon emission as the electron relaxes to its ground state. The emitted photon spectrum would have two peaks, one centred on each transition frequency $\omega_0 \pm 2g$, and corresponding to the two possible nuclear spin states when the decay occurred. Each peak has a width proportional to the transition rate. If the separation between the two transitions is greater than the transition rates, there is little overlap between the $|\uparrow\rangle_n$ and $|\downarrow\rangle_n$ frequency distributions, as shown in Fig. 1. Measuring the energy of the photon would allow us to know which transition has occurred, and thus which state the nuclear spin is in – any coherence is lost, even if the measurement outcome is not recorded. If the frequency distributions of photons emitted from the two different transitions overlap sufficiently, then measuring the frequency of the bath excitation does not allow one to determine which decay occurred, and so the nuclear spin remains in superposition.

In order to extend our results to non-zero temperature, we next derive an approximate MQME for the same system, whose validity we can check by comparing to the exact approach just described. The resulting equation will then allow us to extend our predictions to finite temperature. When deriving a MQME, several key approximations are typically made. Two of these are the Born approximation and the Markov approximation, respectively corresponding to assuming weak system-environment coupling, and short memory times for the bath [2]. In many cases, an additional secular approximation is made, neglecting dissipator terms that are off-diagonal in the energy basis. This assumption is typically justified in quantum-optical systems, where it

is also known as the rotating wave approximation [2], and leads to a Lindblad form for the Liouvillian [20–23]. However, for systems with closely spaced transition frequencies such as the coupled nuclear-electron spins, secularisation, i.e. discounting off-diagonal terms, is not justified. Indeed, secularization predicts that the nuclear coherences will always be zero following electron spin decay, except at $g = 0$, where the nuclear spin is completely isolated anyway. We know both from the exact solution that nuclear coherence can be preserved, and we must therefore avoid secularization here. As discussed elsewhere [24, 25], a microscopically derived Bloch-Redfield equation can yield accurate and physical results for the steady state in such cases.

The Bloch-Redfield equation for the system density matrix $\rho(t)$ following the Born and Markov approximations is [2]:

$$\frac{d\rho}{dt} = \sum_{\{i,j\} \in \{1,2\}} e^{i(\omega_i - \omega_j)t} \left(\Gamma^\uparrow(\omega_i) D_{ij}^\uparrow[\rho] + \Gamma^{\uparrow*}(\omega_j) D_{ji}^{\uparrow\dagger}[\rho] + \Gamma^\downarrow(\omega_j) D_{ij}^\downarrow[\rho] + \Gamma^{\downarrow*}(\omega_i) D_{ji}^{\downarrow\dagger}[\rho] \right), \quad (8)$$

where we have defined $D_{ij}^\uparrow[\rho] \equiv A_i^\dagger \rho A_j - A_j A_i^\dagger \rho$, $D_{ij}^\downarrow[\rho] \equiv A_i \rho A_j^\dagger - A_j^\dagger A_i \rho$ and the transition operators are $A_1 = |\downarrow\downarrow\rangle\langle\uparrow\downarrow|$ and $A_2 = |\downarrow\uparrow\rangle\langle\uparrow\uparrow|$. Here we have introduced the generalizations of the quantity $\Gamma(\omega)$ to non-zero temperatures:

$$\begin{aligned} \Gamma^\downarrow(\omega) &= J(\omega)[n(\omega) + 1] - \frac{i}{\pi} \mathcal{P} \int_0^\infty \frac{J(\nu)[n(\nu) + 1]}{\nu - \omega} d\nu \\ \Gamma^\uparrow(\omega) &= J(\omega)n(\omega) + \frac{i}{\pi} \mathcal{P} \int_0^\infty \frac{J(\nu)n(\nu)}{\nu - \omega} d\nu \end{aligned} \quad (9)$$

where $n(\omega) = [e^{\hbar\omega/k_B T} - 1]^{-1}$ is the Bose-Einstein distribution function, so that at zero temperature $\Gamma^\uparrow(\omega) = 0$.

Solving Eq. (8) yields the following Born-Markov approximated expressions for the nuclear coherences when the electron is spin up and spin down respectively:

$$\begin{aligned} \rho_{\downarrow\downarrow,\downarrow\uparrow}(t) &= [r_{\downarrow\downarrow,\downarrow\uparrow}(e^{-\kappa_- t} - e^{-\kappa_+ t}) + \rho_{\downarrow\downarrow,\downarrow\uparrow}(0)e^{-\kappa_+ t}], \\ \rho_{\uparrow\downarrow,\uparrow\uparrow}(t) &= [r_{\uparrow\downarrow,\uparrow\uparrow}(e^{-\kappa_- t} - e^{-\kappa_+ t}) + \rho_{\uparrow\downarrow,\uparrow\uparrow}(0)e^{-\kappa_+ t}] e^{-4igt}, \end{aligned} \quad (10)$$

where, defining $\gamma^{\uparrow(\downarrow)} = \Gamma^{\uparrow(\downarrow)}(\omega_1) + \Gamma^{\uparrow(\downarrow)*}(\omega_2)$, we have:

$$\begin{aligned} \kappa_\pm &= \frac{1}{2} \left[\gamma^\uparrow + \gamma^\downarrow - 4ig \pm \sqrt{(\gamma^\uparrow + \gamma^\downarrow - 4ig)^2 + 16ig\gamma^\uparrow} \right], \\ r_{\downarrow\downarrow,\downarrow\uparrow} &= \frac{\gamma^\downarrow \rho_{\downarrow\downarrow,\uparrow\uparrow}(0) - (\gamma^\uparrow - \kappa_+) \rho_{\downarrow\downarrow,\downarrow\uparrow}(0)}{\kappa_+ - \kappa_-}, \\ r_{\uparrow\downarrow,\uparrow\uparrow} &= r_{\downarrow\downarrow,\downarrow\uparrow} \left(\frac{\gamma^\uparrow - \kappa_-}{\gamma^\downarrow} \right). \end{aligned} \quad (11)$$

In the dynamics predicted by Eq. (10) there exist two characteristic decay timescales: a fast one governed by

$1/|\text{Re}\{\kappa_+\}|$ and a slow one corresponding to $1/|\text{Re}\{\kappa_-\}|$. At zero temperature, $\gamma_\uparrow = 0$, we find $\kappa_\pm = [\gamma^\downarrow - 4ig](1 \pm 1)/2$, so the slow timescale extends to infinity. Hence, following initialization in state $|\psi(0)\rangle$ we expect a steady state coherence $|\rho_{\downarrow\downarrow,\downarrow\uparrow}(t \rightarrow \infty)| = r_{\downarrow\downarrow,\downarrow\uparrow}$. This quantity is plotted as dashed lines together with the prediction of the exact solution in Fig. 2. The agreement between the two theories is excellent, so long as the electron-bath coupling strength is not too large ($\gamma_0 \ll \omega_0$).

Having established the validity of the MQME we are able to use it to extend our analysis to finite temperature. Here, $1/|\text{Re}\{\kappa_-\}|$ is not zero, but nonetheless the fast and slow timescales can be significantly different — and then there exists a quasi steady state (QSS) once the faster decay process has occurred. In the QSS we find $\rho_{\downarrow\downarrow,\downarrow\uparrow}^{\text{QSS}} = r_{\downarrow\downarrow,\downarrow\uparrow}$ and $\rho_{\uparrow\downarrow,\uparrow\uparrow}^{\text{QSS}} = r_{\uparrow\downarrow,\uparrow\uparrow}$.

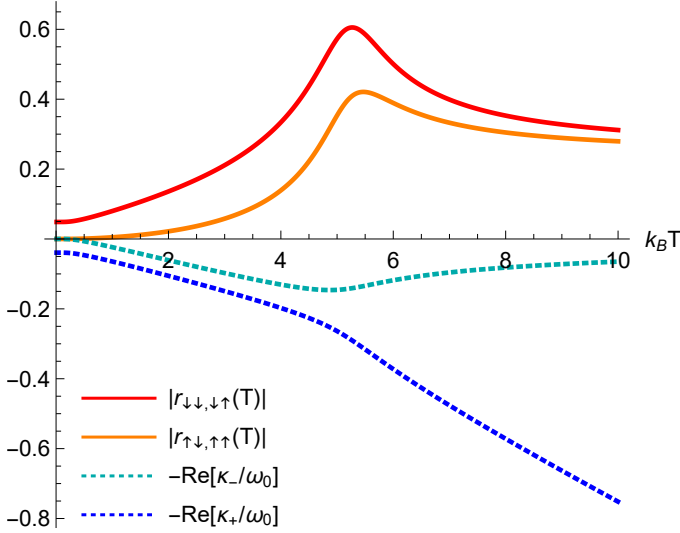


FIG. 3. The quasi steady state nuclear coherences for the upper (orange) and lower (red) electron state, plotted as a function of temperature for $g = 0.1\omega_0$, $\gamma_0 = 0.02\omega_0$. Also plotted are the two characteristic decay rates, $\text{Re}\{\kappa_\pm\}$. A quasi steady state is only observed when $|\text{Re}\{\kappa_-\}|$ is sufficiently small.

The magnitude of the QSS coherences are plotted in Fig. 3 as a function of temperature. Parameters are chosen such that the emission spectrum has well resolved peaks corresponding to the different nuclear spin states at zero temperature. Therefore, even though at very low temperatures a QSS exists it has very small coherence. As the temperature begins to rise, $\gamma^{\uparrow(\downarrow)}$ increases, and becomes comparable to g . This first causes the ratio of fast and slow timescales to approach unity, as both timescales increase by a similar amount. This leads to a regime where a QSS no longer really exists: the values of r here freely exceed the maximum value of ob-

servable coherence of $1/2$. The most remarkable feature occurs as temperature is raised still higher. Here, $\gamma^{\uparrow(\downarrow)} \gg g$, so we may expand κ_\pm in powers of $g/(\gamma^\uparrow + \gamma^\downarrow)$. From this, neglecting the imaginary parts of $\gamma^{\uparrow(\downarrow)}$ we find that the real parts of these expressions scale as $\text{Re}[\kappa_+] \simeq \gamma^\uparrow + \gamma^\downarrow$, $\text{Re}[\kappa_-] \simeq 16g^2\gamma^\uparrow/(\gamma^\uparrow + \gamma^\downarrow)^2$, so the ratio of fast and slow timescales again becomes small and a QSS returns, with coherences at the highest temperatures reaching $|\rho_{\downarrow\downarrow,\downarrow\uparrow}^{\text{QSS}}| = |\rho_{\uparrow\downarrow,\uparrow\uparrow}^{\text{QSS}}| = 1/4$. The maximum nuclear coherence is now shared equally between the two electron states which are now equally populated. These coherences oscillate since the effective magnetic field imposed on the nucleus by the electron is switched for the two electron states. The reduced density matrix of the nuclear spin thus periodically reaches its maximum value of $1/2$, which is *several times larger than its value at zero temperature*. Thus, we must conclude that *heating a hybrid system can stop decoherence*.

In order to observe the protected coherences that we have described, it is necessary to engineer a system whereby the transition spacings are comparable to their linewidths, and which can be tuned. Quantum dots (QDs) doped with a single electron have spin selective optical transitions to trion states, so forming a hybrid spin-photon system. Sweeney *et al.* [26] found that the optical transition spacings in a cavity-QD system were 2.8 times greater than the linewidths. Purcell enhancement in QD systems can broaden linewidths by a factor of 6.7 [27] to produce highly indistinguishable photons, which would allow coherences to survive even at zero temperature.

Closely spaced transitions are also found in NV centres in diamond, already the focus of many quantum computing studies. The NV centre carries an electron spin which can be optically excited via spin selective transitions [28]. The spin sublevel splitting can be tuned in zero magnetic field via an externally applied electric field [28]. By placing the diamond inside a tunable cavity, the emission rate of the NV centre can also be enhanced, increasing transition linewidths [29] — thus providing enough flexibility to observe coherence preservation during decay.

We have shown that decoherence of a system does not apply equally to all its parts, and that a combination of the correct coupling and temperature tuning can preserve the coherence of part of a quantum system. These effects could be exploited in the next generation of hybrid quantum information processing devices.

HMC acknowledges studentship funding from EPSRC under grant no. EP/G03673X/1. PGK acknowledges support from EPSRC (EP/M010910/1). PRE acknowledges funding from SFI (15/IACA/3402). JK acknowledges financial support from EPSRC programs “TOPNES” (EP/I031014/1) and “Hybrid-Polaritonics” (EP/M025330/1).

-
- [1] G. M. Palma, K.-A. Suominen, and A. K. Ekert, *Proc. Roy. Soc. Lond. A* **452**, 567 (1996).
- [2] H. Breuer and F. Petruccione, *The Theory of Open Quantum Systems* (Oxford University Press, 2002).
- [3] M. Schlosshauer, *Rev. Mod. Phys.* **76**, 1267 (2005).
- [4] J. P. Paz and W. H. Zurek, *Phys. Rev. Lett.* **82**, 5181 (1999).
- [5] W. H. Zurek, *Rev. Mod. Phys.* **75**, 715 (2003).
- [6] M. Atatüre, J. Dreiser, A. Badolato, and A. Imamoglu, *Nat. Phys.* **3**, 101 (2007).
- [7] A. J. Ramsay, S. J. Boyle, R. S. Kolodka, J. B. B. Oliveira, J. Skiba-Szymanska, H. Y. Liu, M. Hopkinson, A. M. Fox, and M. S. Skolnick, *Phys. Rev. Lett.* **100**, 197401 (2008).
- [8] M. Schaffry, V. Filidou, S. D. Karlen, E. M. Gauger, S. C. Benjamin, H. L. Anderson, A. Ardavan, G. A. D. Briggs, K. Maeda, K. B. Henbest, F. Giustino, J. J. L. Morton, and B. W. Lovett, *Phys. Rev. Lett.* **104**, 200501 (2010).
- [9] P. Neumann, J. Beck, M. Steiner, F. Rempp, H. Fedder, P. R. Hemmer, J. Wrachtrup, and F. Jelezko, *Science* **329**, 542 (2010).
- [10] Z.-L. Xiang, S. Ashhab, J. Q. You, and F. Nori, *Rev. Mod. Phys.* **85**, 623 (2013).
- [11] D. Marcos, M. Wubs, J. M. Taylor, R. Aguado, M. D. Lukin, and A. S. Sørensen, *Phys. Rev. Lett.* **105**, 210501 (2010).
- [12] J. J. L. Morton and B. W. Lovett, *Ann. Rev. Cond. Matter Phys.* **2**, 189 (2011).
- [13] G. Kurizki, P. Bertet, Y. Kubo, K. Mølmer, D. Petrosyan, P. Rabl, and J. Schmiedmayer, *Proc. Natl. Acad. Sci.* **112**, 201419326 (2015).
- [14] G. W. Morley, P. Lueders, M. Hamed Mohammady, S. J. Balian, G. Aeppli, C. W. M. Kay, W. M. Witzel, G. Jeschke, and T. S. Monteiro, *Nat. Mater.* **12**, 103 (2012).
- [15] N. Zhao and J. Wrachtrup, *Nat. Mater.* **12**, 97 (2013).
- [16] M. Zhong, M. P. Hedges, R. L. Ahlefeldt, J. G. Bartholomew, S. E. Beavan, S. M. Wittig, J. J. Longdell, and M. J. Sellars, *Nature* **517**, 177 (2015).
- [17] A. Bienfait, J. J. Pla, Y. Kubo, X. Zhou, M. Stern, C. C. Lo, C. D. Weis, T. Schenkel, D. Vion, D. Esteve, J. J. L. Morton, and P. Bertet, *Nature* **531**, 74 (2016).
- [18] V. Weisskopf and E. Wigner, *Zeitschrift für Physik* **63**, 54 (1930).
- [19] B. Vacchini and H.-P. Breuer, *Phys. Rev. A* **81**, 042103 (2010).
- [20] G. Lindblad, *Comm. Math. Phys.* **48**, 119 (1976).
- [21] R. Dümcke and H. Spohn, *Z. Phys. B* **34**, 419 (1979).
- [22] J. Jeske, D. J. Ing, M. B. Plenio, S. F. Huelga, and J. H. Cole, *J. Chem. Phys.* **142**, 064104 (2015).
- [23] P. Pearle, *Europ. J. Phys.* **33**, 805 (2012), arXiv:1204.2016.
- [24] J. Jeske, D. Ing, M. B. Plenio, S. F. Huelga, and J. H. Cole, *J. Chem. Phys.* **142**, 064104 (2015).
- [25] P. R. Eastham, P. Kirton, H. M. Cammack, B. W. Lovett, and J. Keeling, *Phys. Rev. A* **94**, 012110 (2016).
- [26] T. M. Sweeney, S. G. Carter, A. S. Bracker, M. Kim, C. S. Kim, L. Yang, P. M. Vora, P. G. Brereton, E. R. Cleveland, and D. Gammon, *Nat. Photon.* **8**, 442 (2014), arXiv:1402.4494.
- [27] S. Weiler, A. Ulhaq, S. M. Ulrich, S. Reitzenstein, A. Löffler, A. Forchel, and P. Michler, *Phys. Stat. Solidi B* **248**, 867 (2011).
- [28] E. Bourgeois, A. Jarmola, P. Siyushev, M. Gulka, J. Hruby, F. Jelezko, D. Budker, and M. Nesladek, *Nat Commun* **6**, 8577 (2015).
- [29] S. Johnson, P. R. Dolan, T. Grange, A. A. P. Trichet, G. Hornecker, Y. C. Chen, L. Weng, G. M. Hughes, A. A. R. Watt, A. Auffèves, and J. M. Smith, *New J. Phys.* **17**, 122003 (2015).